Fossilization and degradation of archaeal intact polar tetraether lipids in deeply-buried marine sediments (Peru Margin)

Sabine K. Lengger[*,#]*, Ellen C. Hopmans, Jaap S. Sinninghe Damsté and Stefan Schouten*

Department of Marine Organic Biogeochemistry, Royal NIOZ Netherlands Institute for Sea Research, P. O. Box 59, 1790AB Den Burg, Texel, The Netherlands.

[#]Present address: Petroleum & Environmental Geochemistry Group, Biogeochemistry Research Centre, Plymouth University, Drake Circus, Plymouth, Devon, PL4 8AA, UK. [*]Corresponding author. Tel. +4417525584556, e-mail: sabine.lengger@plymouth.ac.uk
as published in: *Geobiology* **12** (2014), 212-220, doi: 10.1111/gbi.12081

Abstract

Glycerol dibiphytanyl glycerol tetraether (GDGT) lipids are part of the cellular membranes of Thaumarchaeota, an archaeal phylum composed of aerobic ammonia oxidizers, and are used in the paleotemperature proxy TEX_{86}. GDGTs in live cells possess polar head groups and are called intact polar lipids (IPL-GDGTs). Their transformation to core lipids (CL) by cleavage of the head group was assumed to proceed rapidly after cell death but it has been suggested that some of these IPL-GDGTs can, just like the CL-GDGTs, be preserved over geological timescales. Here, we examined IPL-GDGTs in deeply buried (0.2-186 mbsf, ~2.5 Myr) sediments from the Peru Margin. Direct measurements of the most abundant IPL-GDGT, IPL-crenarchaeol, specific for Thaumarchaeota, revealed depth profiles which differed per head group. Shallow sediments (<1 mbsf) contained IPL-crenarchaeol with both glycosidic- and phosphate headgroups, as also observed in thaumarchaeal enrichment cultures, marine suspended particulate matter and marine surface sediments. However, hexose, phosphohexose-crenarchaeol is not detected anymore below 6 mbsf (~7 kyr), suggesting a high lability. In contrast, IPL-crenarchaeol with glycosidic head groups is preserved over time scales of Myr. This agrees with previous analyses of deeply buried (>1 m) marine sediments, which only reported glycosidic and no phosphate-containing IPL-GDGTs. TEX_{86} values of CL-GDGTs did not markedly change with depth, and the TEX_{86} of IPL-derived GDGTs decreased only when the proportions of monohexose- to dihexose-GDGTs changed, likely due to the enhanced preservation of the monohexose GDGTs. Our results support the hypothesis that in situ GDGT production and differential IPL degradation in sediments is not substantially affecting TEX_{86} paleotemperature estimations based on CL GDGTs and indicate that likely only a small amount of IPL-GDGTs present in deeply buried sediments is part of cell membranes of active Archaea. The amount of archaeal biomass in the deep biosphere based on these IPLs may have been substantially overestimated.

1. INTRODUCTION

Archaea form the third domain of life, as classified by Woese & Fox (1977). One of the characteristics that distinguish them from bacteria and eukaryotes is their membrane lipid composition, consisting of isoprenoid chains linked to glycerol moieties via ether bonds. Many archaea produce glycerol dibiphytanyl glycerol tetraether lipids (GDGTs; Langworthy, 1977; Koga & Nakano, 2008). These include a GDGT containing two acyclic biphytane moieties (GDGT-0; see Fig. 1 for structures), and GDGTs in which the biphytanes contain cyclopentane moieties formed by internal cyclization (e.g. GDGT-1 to -3). Crenarchaeol, which contains a cyclohexane moiety, and the crenarchaeol regio-isomer (Fig. 1) are GDGTs produced exclusively by Thaumarchaeota (Sinninghe Damsté *et al.*, 2002b; 2012). In live cells, GDGTs are present as intact polar lipids (IPLs), i.e. with polar head groups such as hexose- or/and phosphate groups (Fig. 1b; e.g. Koga & Morii, 2005 and references therein). These IPLs are, upon cell death, presumably transformed by cleavage of the head group into recalcitrant core lipids (CLs) GDGTs (Schouten *et al.*, 2013 and references cited therein), whose relative abundances are used in the temperature proxy TEX_{86} (Schouten *et al.*, 2002). In enrichment cultures of Thaumarchaeota, IPL-GDGTs mainly occur as monohexose (MH)-, dihexose (DH)-, phospho- and hexose, phosphohexose (HPH)-GDGTs (Pitcher *et al.*, 2010; 2011a; Schouten *et al.*, 2008; Sinninghe Damsté *et al.*, 2012). These IPLs are also observed in suspended particulate matter in the water column (Pitcher *et al.*, 2011b; Schouten *et al.*, 2012; Schubotz *et al.*, 2009) and in marine sediments (Lengger *et al.*, 2012a; Schubotz *et al.*, 2009).

IPLs have been used as biomarkers for live microbes in studies of deeply buried sediments, the so-called "deep biosphere" (Biddle *et al.*, 2006; Lipp *et al.*, 2008; Lipp & Hinrichs, 2009). These studies have shown, in general, that archaeal IPLs dominate over bacterial IPLs (the latter representing generally <10% of total IPLs) in marine sediments at depths >1 mbsf. However, the IPL-GDGTs reported in these sediments consisted only of glycolipids, and several studies indicate that these are less suitable for use as biomarkers for live archaea. Experiments conducted by Harvey *et al.* (1986) have shown that archaeal ether lipids with a glycosidic head group are not degraded as rapidly as eukaryotic phosphoester lipids. Schouten *et al.* (2012) showed that water column profiles of crenarchaeol with a MH-head group in the Arabian Sea were

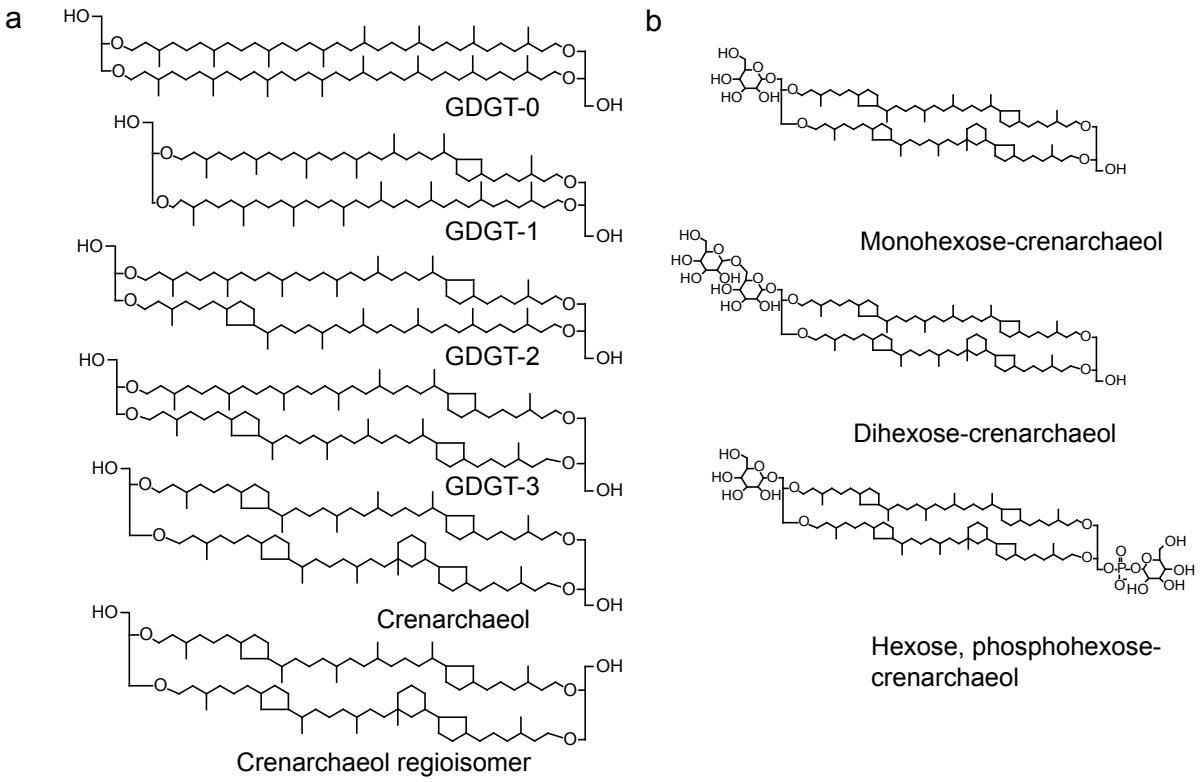

Figure 1. Structures of core lipid (a) and intact polar lipid (b) GDGTs.

not showing any resemblance to thaumarchaeal DNA or RNA profiles, suggesting they do not reflect live archaea. Lengger *et al.* (2012a) demonstrated that MH- and dihexose (DH)-crenarchaeol were only marginally degraded over a timespan of several kyr in Arabian Sea sediments when compared to HPH- crenarchaeol. Logemann *et al.* (2011) conducted degradation experiments over 100 days, in which IPL-GDGTs, including those with a phosphate head group, did not degrade at all. Indeed, recent degradation experiments conducted by Xie *et al.* (2013), suggested turnover times of glycolipids of more than 10 kyr . Finally, even within glycosidic GDGTs different degradation rates are observed, i.e., MH-crenarchaeol was reduced an order of magnitude less by post-depositional oxidation than DH-crenarchaeol (Lengger *et al.*, 2013). This relatively recalcitrant nature of glycolipids does not only hold true for archaeal glycolipids, but extends to other types of lipids as well. For example, Bauersachs *et al.* (2010) have shown in Eocence sediments that glycolipids from heterocystous cyanobacteria were preserved for ca. 40 Myr. It is thus questionable how much of the IPL-GDGTs buried in deep marine sediments is part of live archaeal cells, and how much is fossil (Schouten *et al.*, 2010; Xie *et al.*, 2013).

Although the above studies show slow degradation of glycosidic GDGTs over time spans of up to kyrs, less is known about phospholipid-GDGTs, which are major IPLs in all enriched Thaumarchaeota to date (Pitcher *et al.*, 2010; 2011a; Schouten *et al.*, 2008; Sinninghe Damsté *et al.*, 2012). Lipp & Hinrichs (2009) did not report phospholipid-GDGTs in the sediments they analyzed. However, Schouten *et al.* (2010) predicted that the supposedly more labile IPLs containing a phosphate head group (e.g. hexose, phosphohexose (HPH)-GDGTs) would disappear rapidly with sediment age/depth compared to strictly glycosidic IPL GDGTs, explaining why only glycosidic GDGTs are detected in deeply buried marine sediment. Indeed, Lengger *et al.* (2012a) showed that the concentration of HPH-crenarchaeol decreased rapidly in surface sediments, although it was still detected in sediments of several kyrs old. However, to the best of our knowledge, no study has yet investigated the behavior of phospho-GDGTs, including HPH-crenarchaeol, over much longer time scales, i.e. millions of years, in order to test the hypothesis of Schouten *et al.* (2010).

To this end, we re-investigated deeply buried marine sediments from site 1229 of ODP leg 201 (Peru Margin), which have previously been used by Lipp & Hinrichs (2009), together with sediments from other ODP cores, to determine concentrations of CL- and IPL-derived GDGT as well as individual IPL-crenarchaeol species, including those with an HPH-head group, over a large depth (186 mbsf) and time (2.5 Myr) interval. The results are interpreted to reflect preferential degradation of certain IPL-species originally present in the surface sediments. We also discuss the consequence of these findings for TEX_{86} palaeothermometry.

2. Materials and methods

2.1. Site description

The sediments were recovered during ODP Leg 201 from the Peru Margin at site 1229, a leg specifically designed for microbial investigations (D'Hondt *et al.*, 2003). The samples investigated were from holes A, D and C at depths from 0 to 186 m (Table 1). The samples were directly frozen after recovery and stored at -20°C. The ages of the sediments were estimated based on reported sedimentation rates of 32.3 cm . kyr^{-1} for the top 0-20 cm, 98.1 cm . kyr-1 for 21-230 cmbsf and 5.1 cm . kyr^{-1} for 231 to 270 cmbsf, which is interpreted as the base of the Holocene (D'Hondt *et al.*, 2003). Below, an average sedimentation rate of 7.98 cm . kyr^{-1} was calculated using the Pleistocene/Pliocene transition as stratigraphic marker (2,588 kyrs), located at 190 mbsf (D'Hondt *et al.*, 2003). Freeze-dried sediments were analyzed for organic carbon concentrations (C_{org}). The freeze-dried sediment

Table 1. Sample details, absolute depths, sedimentation rates, age and organic carbon content at station 1229 (Leg 201). Sedimentation rates used taken from Skilbeck & Fink (2006) and D'Hondt et al. (2003). Interval denotes the part of the core section that was used for analysis.

Hole	Core	Section	Interval [cm]	Sampling depth [mbsf]	Age [kyr]	C_{org} [%]
D	1	1	20-25	0.2	0.6406	5.9
D	1	1	82-92	0.8	0.841	7.1
D	1	4	120-125	6.0	281	4.8
A	2	2	10-15	6.5	288	2.8
A	2	2	137-147	7.8	304	3.2
A	2	5	50-60	11.4	350	1.8
A	4	2	10-15	25.5	526	6.8
A	4	5	69-79	30.6	590	6.9
A	5	5	10-15	39.5	702	2.4
D	6	1	130-135	41.1	722	3.9
A	6	2	99-109	42.4	738	2.3
D	7	4	89-94	54.7	892	1.2
C	8	2	0-7	60.4	964	0.9
A	8	5	50-60	65.4	1026	1.0
A	10	2	55-65	81.5	1228	3.9
D	12	2	79-89	85.6	1279	3.0
D	12	3	74-79	87.1	1298	4.0
D	13	2	20-25	89.0	1322	1.2
A	12	3	65-75	102.1	1486	3.0
A	18	2	70-80	157.6	2182	0.9

was acidified overnight with 2N HCl, subsequently washed with bidistilled H_2O and the water was removed by freeze-drying. The decalcified sediments were measured on a Flash EA 1112 Series (Thermo Scientific) analyzer coupled via a Conflo II interface to a Finnigan Deltaplus mass spectrometer. Standard deviations from three measurements ranged from 0.01 to 0.2 % TOC.

2.2. Sediment extraction and IPL-CL-GDGT separation

Aliquots (1-2 g) of freeze-dried sediment were extracted with a modified Bligh and Dyer procedure as described by Lengger *et al.* (2012b). The extracts were stored at -20°C.

One aliquot of extract was directly analyzed by HPLC/ESI-MS^2 for intact polar lipids (IPLs) containing crenarchaeol, while another aliquot was fractionated over a silica column in order to separate the IPLs from the core lipids (CL) following the procedure of Oba *et al.* (2006), modified by Pitcher *et al.* (2009) and Lengger *et al.* (2012b). The core lipid fractions were dried and 0.1 μg C_{46}-GDGT internal standard (Huguet *et al.*, 2006) was added. To the intact polar lipid fractions 0.1 μg internal standard was added and an aliquot of 3 mL was transferred to a vial, dried and stored frozen for quantification of core lipids which eluted in the intact polar lipid fraction ("carry over"). These were typically <2% of the GDGTs present in CL fraction or 10% of GDGTs present in the IPL fraction, and thus negligible. The remaining IPL fraction was dried and hydrolyzed to release CL-GDGTs according to Pitcher *et al.* (2009). This yielded the IPL-derived GDGTs, which were quantified using a C_{46} GDGT internal standard, with a limit of detection of 0.05 ng injected on column (Huguet *et al.*, 2006).

2.3. HPLC/APCI-MS, HPLC/ESI-MS^2 and data analysis

Analysis of CL-GDGTs and IPL-derived GDGTs by HPLC/APCI-MS and calculation of TEX_{86} was carried out as described previously (Schouten *et al.*, 2012). Reproducibility for TEX_{86} values is typically < 0.02, corresponding to errors of < 1 °C. Temperatures were calculated using the calibrations according to Kim *et al.* (2010) for TEX_{86}^{H}. Intact polar lipids with a crenarchaeol core (Fig. 1c) were directly analyzed by HPLC/ESI-MS^2 using a specific selected reaction monitoring method (SRM; Pitcher *et al.*, 2011b). No direct absolute quantification of IPLs was possible due to a lack of standards. Therefore, response areas per g sediment are reported. The method has been reported to detect amounts as low as 0.01 ng/g sediment dw, equating to ~ 7 pg injected on the column (Lengger *et al.*, 2013). Performance of the ESI-MS^2 was monitored by repeat injections of an extract of Arabian Sea sediment (obtained from Lengger *et al.*, 2012b), typically after each 8 sample runs. Duplicate injections yielded relative standard deviations of the areas (on average 2%). A principal component analysis was conducted on the concentrations of organic carbon, CL- and IPL-derived GDGTs and abundances of IPL-crenarchaeol species, using the software PAST (Hammer *et al.*, 2001).

3. Results

Organic carbon concentrations ranged from 0.2 to 6.9 %, with a tendency to decrease with depth, but with large scatter (Table 1). This was also observed for concentrations of CL-GDGT-0, which ranged from 0.1 to 21 μg . g sed dw^{-1}, of CL-crenarchaeol, ranging from 0.2 to 35 μg . g sed dw^{-1}, and of the minor isoprenoid GDGTs (minor iGDGTs, the sum of GDGT-1, -2, -3 and crenarchaeol regio-isomer, which are used in the TEX_{86}), ranging from 0.04 to 6 μg . g sed dw^{-1} (Fig. 2a). When concentrations were normalized to Corg, only minor changes in concentrations were observed: they ranged between <0.1 and 0.5 μg . g C_{org}^{-1} for the minor iGDGTs, 0.2 and 1.3 for GDGT-0 and <0.1 and 2.1 for crenarchaeol (Fig. S1a). When the relative distribution is considered, CL-GDGT-0 slightly increased proportionally with depth (from 27 to 41 %), while crenarchaeol decreased (from 61 to 47 %) (Fig. 2a; right panel).

IPL-derived GDGT concentrations, i.e. GDGTs in the IPL-fraction released by hydrolytic cleavage of head groups, were consistently lower than the CL-GDGT concentrations. Concentrations ranged from 0.05 to 3.2 μg . g sed dw^{-1} for GDGT-0, 0.03 to 2.2 μg . g sed dw^{-1} for crenarchaeol, and 0.01 to 2.8 μg . g sed dw^{-1} for the IPL-derived minor iGDGTs, with a tendency to decrease with depth, but again with large scatter (Fig. 2b). The proportion of GDGT-0 in the IPL-GDGTs was higher than in the CL-GDGTs (38 %), and increased with depth to 52 %, while the minor iGDGTs decreased from 26 to 14 % and crenarchaeol from 36 to 33% (Fig. 2b). When concentrations were normalized on TOC, no particular depth trend was observed, and concentrations ranged from <0.01 to 0.012 for the minor iGDGTs and crenarchaeol, and from 0.01 to 0.2 for GDGT-0 (Fig. S1b).

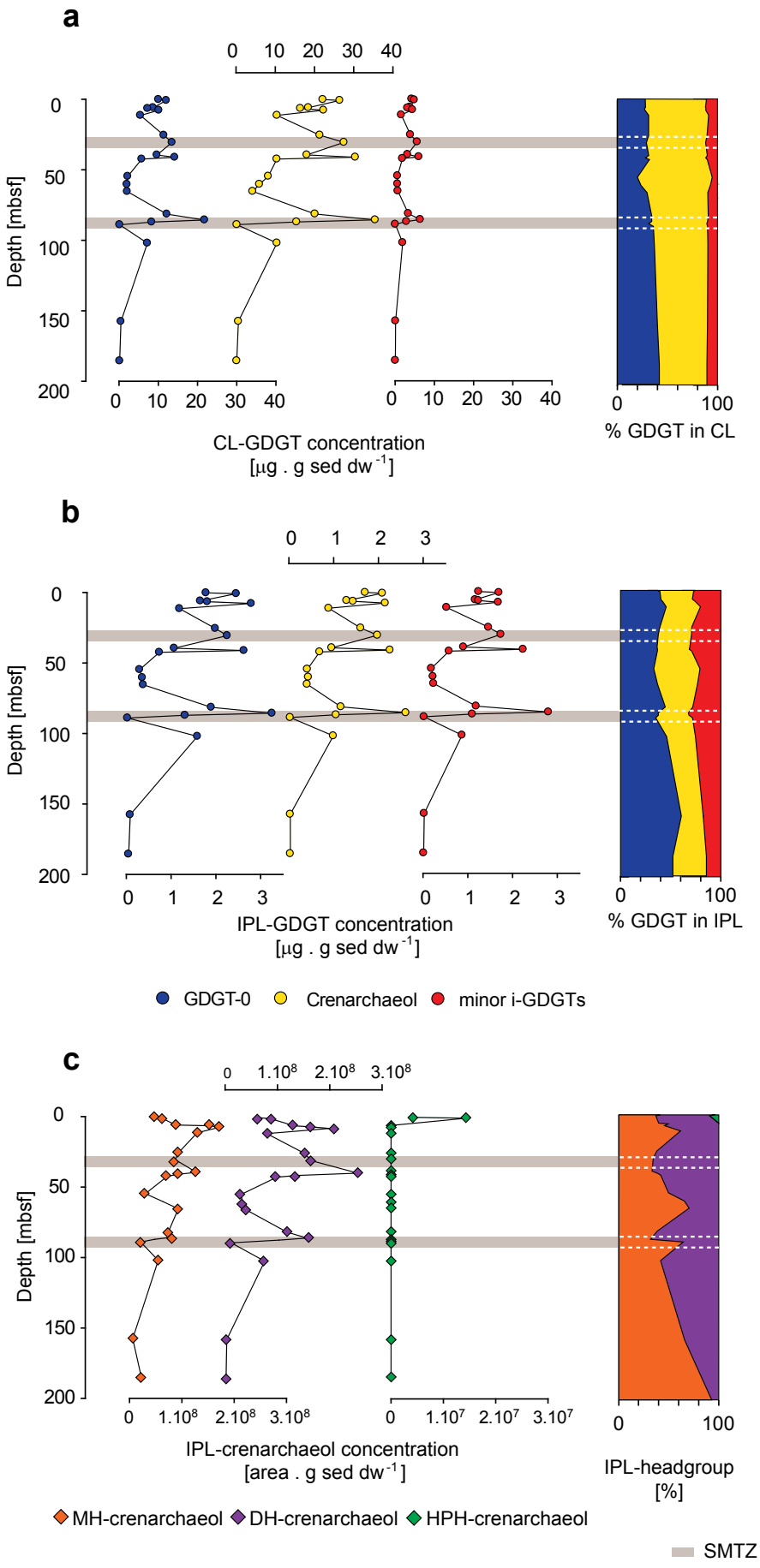

Figure 2. Concentrations vs. depth (mbsf) of (a) CL-GDGTs in µg . g sed dw^{-1}, (b) IPL-derived GDGTs in µg . g sed dw^{-1}, (c) IPL-crenarchaeol with MH-, DH- and HPH-headgroups (in area . g sed dw^{-1}). Coloured area graphs show GDGT distributions as a percentage of the total sum.

The MH- and DH-crenarchaeol directly measured by HPLC-ESI-MS^2, showed a general decrease in concentration with depth, from 108 down to almost 106 area . g sed dw^{-1} for both IPL-crenarchaeol species, though again with large scatter (Fig. 2c), while abundances of HPH-crenarchaeol decreased rapidly with depth and were below detection limit under 6 mbsf. The proportion of DH crenarchaeol compared to MH-crenarchaeol decreased with depth (Fig. 2c). Normalized on TOC, MH- and DH-crenarchaeol ranged between 104 and 107 area . g C_{org}^{-1} and HPH-crenarchaeol decreased from 103 area . g C_{org}^{-1} to below the detection limit (Fig. S1c).

Principal component analysis (Fig. S2) revealed that the first component (PC1) explained 81 % of the variance in GDGT distributions, with the second component (PC2) explaining 9% of the variance. The samples from all depths varied only over PC1, except for 0.2 and 0.8 mbsf which were different from all the other depths on PC2. The loadings of all variables on PC1 were plotting similar to C_{org}, suggesting their covariance with C_{org}, while PC2 was defined by the concentration of HPH-crenarchaeol relative to MH- and DH-crenarchaeol (Fig. S2b).

The TEX_{86} of the CL-GDGTs ranged from 0.51 to 0.62 with no specific depth trend, while the TEX_{86} of IPL-derived GDGTs was slightly higher and ranged from 0.62 to 0.74 with a sharp decline below 102 mbsf (Fig. 3a).

4. Discussion

4.1 Degradation of IPL-GDGTs

Our results show that both CL- and IPL-derived GDGT-concentrations as well as TOC were decreasing with depth, although with large scatter. The large scatter is most probably due to the variations in depositional environment, due to the large timescales investigated (Myr). The Peru Margin is characterized by high productivity, controlled by coastal upwelling, and possesses a pronounced oxygen minium zone (OMZ), which has varied over time (cf. Gutiérrez *et al.*, 2011; Powell *et al.*, 1990), leading to changes in organic matter fluxes, oxygen concentrations, oxygen exposure time and, consequently, organic carbon and biomarker preservation efficiency (cf. Hartnett *et al.*, 1998; Hedges & Keil, 1995; Sinninghe Damsté *et al.*, 2002a). These different degrees of oxygen exposure time (OET) can potentially have a large effect on both the TOC and the concentration of biomarker lipids. Indeed, the principal component analysis (Fig. S2) suggests a covariance of the concentrations of CL- and IPL-GDGTs with C_{org}. This suggests that preservation of CL- and IPL-GDGTs is determined by similar factors as C_{org}.

Direct measurements of IPL-crenarchaeol with different head groups allowed us to investigate the prediction of Schouten *et al.* (2010) on the different degradation behavior of phospholipids versus glycolipids. At depths > 6 mbsf only glycosidic crenarchaeol was detected (MH- and DH-crenarchaeol), in agreement with the results obtained by Lipp and Hinrichs (2009). However, at shallow depths also HPH-crenarchaeol was present, a phospholipid which shows a rapid decrease with depth and is undetectable below 6 mbsf, i.e. within <7 kyrs. This confirms the prediction of Schouten *et al.* (2010) that HPH-GDGTs are degraded faster than IPLs with glycosidic head groups, and the observations of Lengger *et al.* (2012a) who observed a fast decrease of HPH-crenarchaeol over the upper 30 cm of surface sediments in the Arabian Sea. The depth profile of HPH-crenarchaeol is in strong contrast to that of the glycosidic crenarchaeol-IPLs, which show a depth trend similar to that of TOC and CL-GDGTs (Fig. 2c, Fig. S2). The apparent persistence of glycosidic GDGTs compared to HPH-GDGTs could either be due to archaea at depth producing only glycosidic GDGTs and no HPH-GDGTs, or be due to their better preservation. Several arguments are in disfavor of a significant contribution of in situ production to sedimentary MH- and DH-GDGTs: Firstly, crenarchaeol has, until now, only been found in Thaumarchaeota performing the aerobic oxidation of ammonia and not in anaerobic archaea, which would be expected in anoxic, deeper sediments. Secondly, calculations conducted by Schouten *et al.* (2010) showed that IPL-abundance clearly exceeded the amount expected from the number of archaeal cells present in these sediments by two orders of magnitude, indicating a substantial fossil contribution. Xie *et al.* (2013) recently showed that growth rates of archaea in subsurface sediments were extraordinarily low, thus rendering a substantial contribution of in situ production highly unlikely. Additionally, production of IPL-crenarchaeol and other IPL-GDGTs in the sediment would likely alter the distribution of GDGTs in the sediment, especially at depths where a strong archaeal contribution would be expected, i.e. in the sulfate-methane transition zones (SMTZs) reported at this site at 30 and 88 mbsf (Biddle *et al.*, 2006). According to Weijers *et al.* (2011), a strong increase in GDGT-2 / crenarchaeol would be expected in association with the presence of archaeal methanotrophic (i.e. ANME-1) communities. However, this is not the case in the SMTZ here (Fig. 3b), except for a small increase at 80 m depth, which is, however, only observed in the IPL-fraction and not in the CL-fraction. In any case, this imprint was not transferred to the underlying zones, in agreement with the observations of Weijers *et al.* (2011). This all suggests a relatively low contribution of in situ production to the sedimentary pool of GDGTs.

One observation is that MH-crenarchaeol concentrations increase with depth relative to DH-crenarchaeol (Fig. 2c), possibly due to a better preservation of the MH-crenarchaeol. The deeper sediments are also those containing the lowest amounts of organic carbon and were likely deposited in times of lower OMZ intensity and thus subjected to longer OET. It has been shown that DH-crenarchaeol is more labile under oxic conditions than MH-crenarchaeol (Lengger *et al.*, 2013), and this may be the reason for its decrease in proportion. However, another possibility is a past change in pelagic Thaumarchaeota communities producing relatively more MH-crenarchaeol.

Our findings have implications for the use of IPL-GDGTs as biomarkers for live Archaea, especially for the use of glycosidic IPL-GDGTs in deeply buried sediments. According to our results, a large amount of these glycosidic IPLs is most probably fossil in nature and is not representative of the actual amount of live and active archaeal cells. Rather, it is advisable to focus on IPLs with more labile headgroups such as phospholipids as markers for living archaea and bacteria.

4.2 Impact of IPL-GDGT degradation on TEX_{86}

IPL-GDGTs in sediments are of interest because their production or differential degradation can affect GDGT-based proxies. While, as previously shown, the TEX_{86} is not affected by sedimentary processes over short time scales (<10 yrs, Lengger *et al.*, 2012a; 2013), this has not yet been investigated over larger timescales. The TEX_{86} of the CL-GDGTs varied from 0.51 to 0.62 (Fig. 3a), likely reflecting the substantial changes in sea surface temperature (Schouten *et al.*, 2002) over a time period stretching

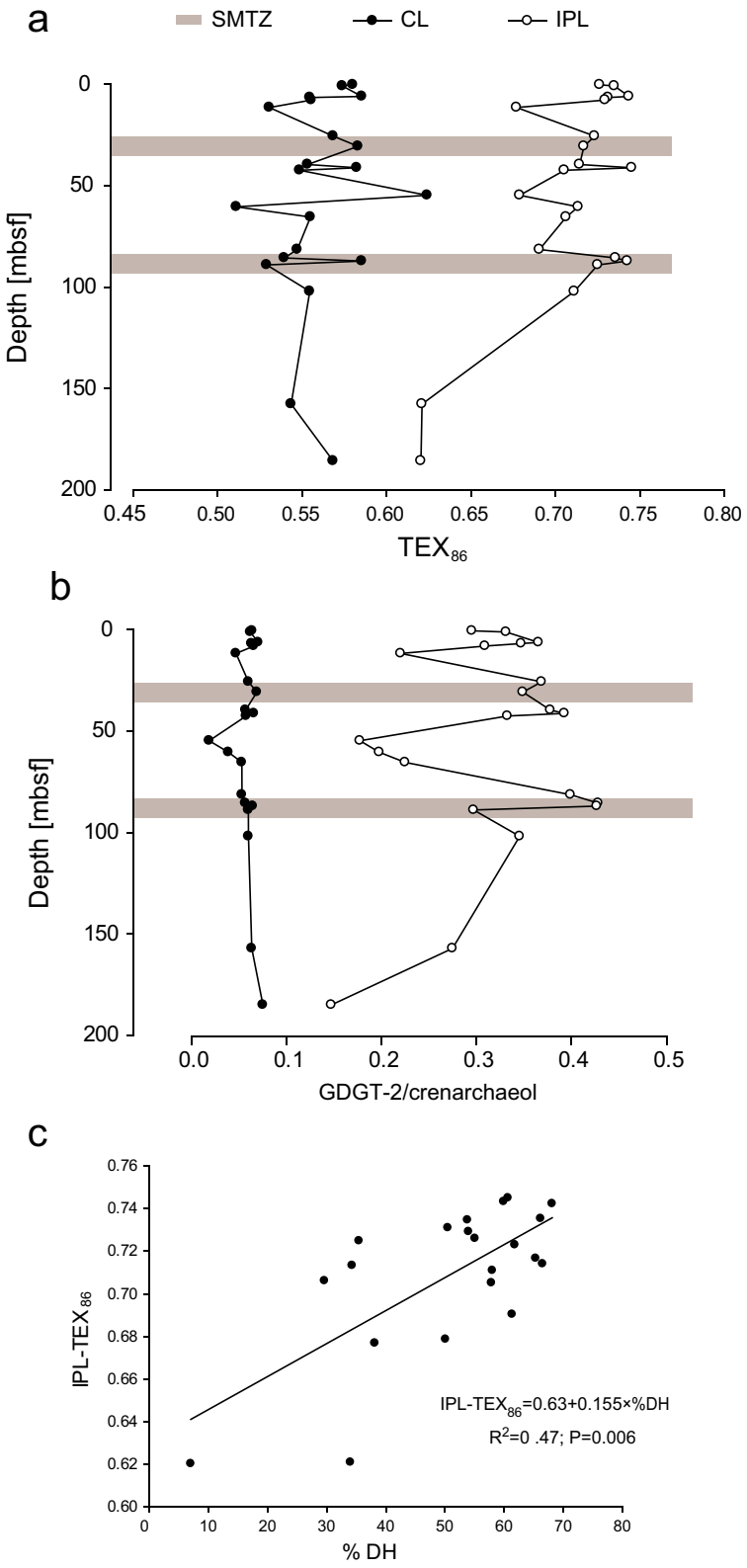

Figure 3. (a) CL- and IPL-derived TEX_{86} values plotted against depth in mbsf, (b) GDGT-2/crenarchaeol ratio of IPL-derived and CL-GDGTs and (c) IPL-derived TEX_{86} as a function of % DH-crenarchaeol.

to the late Pliocene (D'Hondt *et al.*, 2003) which includes glacial-interglacial cycles (the dating /sampling of this core is not extensive enough to locate such cycles; cf. Skilbeck & Fink, 2006). IPL-derived GDGTs have TEX_{86} values higher than the CL-GDGTs and ranged from 0.62 to 0.74 (Fig. 3a). This is similar to what was observed previously in deeply buried sediments analyzed by Liu *et al.* (2011) who reported a correlation between TEX_{86} values obtained from IPL-derived GDGTs and CL-GDGTs, and Lengger *et al.* (2012a) in Arabian Sea surface sediments. However, we did not find such a correlation (R2=0.013; P=0.62; Fig. S3). The reason for this might be the limited range of TEX_{86} values (0.1 units compared to 0.4 units in the data presented by Liu *et al.*, 2011), and scatter may have masked the correlation. The higher TEX_{86} values of IPL-derived GDGTs may be due to the fact that core lipids are not distributed evenly over the IPLs. Lengger *et al.* (2012a) suggested that the higher TEX_{86} of IPL-GDGTs versus CL-GDGTs is due to preferential degradation of HPH-GDGTs, which generally have lower TEX_{86} values, leaving mainly GDGTs with higher TEX_{86} values, such as DH-GDGTs, in the IPL-fraction. This is probably also the case here, as only glycosidic GDGTs remain in the deeper sediment (Fig. 2c), in agreement with Lipp *et al.* (2008), Lipp & Hinrichs (2009) and Liu *et al.* (2011) who also found only glycosidic GDGTs at depth. Indeed, a trend to lower TEX_{86} values from 0.2 to 6.5 m depth is accompanied by the disappearance of the HPH-crenarchaeol. However, the change is relatively small, which is possibly due to the HPH-GDGTs being present in low amounts compared to the MH- and DH-GDGTs even in the shallow sediment at 0.2 mbsf. This would be consistent with the reported rapid decline of the HPH-crenarchaeol abundance in the surface sediments (0-24 cmbsf) of the Arabian Sea (Lengger *et al.*, 2012a).

A strong decrease in TEX_{86} from 0.71 to 0.62 was observed for the IPL-derived GDGTs but not for the CL-GDGTs between 102 and 158 mbsf (Fig. 3a). In this interval, the DH-crenarchaeol concentrations were decreasing faster than the MH-crenarchaeol concentrations (Fig. 2c). In fact, the proportion of DH-crenarchaeol to summed IPL-crenarchaeol changed between these sediments from 58 to 31% and then decreased further to 7% in the deepest sediment (1_{86} mbsf; Fig. 2c). It is likely that this degradation pattern is more dependent on the head group than on the core lipid (cf. Lengger *et al.*, 2013), and thus this proportional change in MH- versus DH-head group was likely occurring in all IPL-GDGTs. DH-GDGTs have a higher TEX_{86} value than MH-GDGTs in all settings and organisms where this has been investigated (Lengger *et al.*, 2012a; 2013; Pitcher *et al.*, 2010; 2011a; Schouten *et al.*, 2008; 2012; Schubotz *et al.*, 2009; Sinninghe Damsté *et al.*, 2012; Zhu *et al.*, 2013). Thus, it may well be that the change in TEX_{86} was due to the proportional change in DH-GDGTs versus MH-GDGTs. Indeed, a significant correlation (R^2 = 0.47; P=0.006) was observed between TEX_{86} of IPL-GDGT and the % DH crenarchaeol (Fig. 3c). It is thus likely that the IPL-derived TEX_{86} value depends, apart from the original pelagic signature, also on the relative degradation rates of types of IPL present. Schouten *et al.* (2012) found a similar correlation in suspended particulate matter in the Arabian Sea water column, although with a much more gradual slope ($IPL\text{-}TEX_{86}$ = 0.628 + 0.0035 × %DH; R^2=0.40). A similar phenomenon was observed in the post-depositional oxidation of marine sediment from the Madeira Abyssal Plain, i.e. the TEX_{86} value changed with a changing proportion of DH-crenarchaeol (Lengger *et al.*, 2013). As stated above, though, the CL-GDGT TEX_{86} does not seem to be impacted by this effect, agreeing with previous observations. It is thus likely that the IPL-derived TEX_{86} value depends, in addition to the original signature, also on the relative degradation rates of types of IPL present.

5. Conclusions

The analysis of deeply buried sediments retrieved from the Peru Margin showed that HPH-crenarchaeol was rapidly degraded in contrast to other IPL-crenarchaeol species, indicating its labile nature compared to glycosidic crenarchaeol-IPL-GDGTs, and was reduced to amounts below detection limits within less than 7 kyr. This higher degradability makes it a suitable biomarker for living organisms in contrast to glycosidic IPL-GDGTs. TEX_{86} values of CL-GDGTs did not show any obvious depth / age trends, however, IPL-derived GDGTs showed a strong decrease of TEX_{86} in the deepest/oldest sediments coinciding with low TOC values. In agreement with previous studies, this could be due to the faster degradation of DH-crenarchaeol compared to the MH-crenarchaeol. Indeed, DH-crenarchaeol percentages showed a correlation with IPL-derived TEX_{86}. Differential degradation, however, in spite of affecting IPL-derived TEX_{86} values, does not have an impact on $CL\text{-}TEX_{86}$.

Acknowledgements. We thank Dr. Ann Pearson and two anonymous reviewers for constructive comments which substantially improved the manuscript. We thank D. J. Rush and A. Mets for analytical assistance. This research used samples from the Ocean Drilling Program (ODP).The ODP was sponsored by the U.S. National Science Foundation and participating countries under management of Joint Oceanographic Institutions (JOI) Inc. S. K. L. was partly funded by a studentship granted to S. S. by the Darwin Institute for Biogeosciences. This is publication nr. DW-2014-1001 of the Darwin Institute for Biogeosciences.

REFERENCES

Bauersachs T, Speelman EN, Hopmans EC, Reichart G-J, Schouten S, Sinninghe Damsté JS (2010) Fossilized glycolipids reveal past oceanic N_2 fixation by heterocystous cyanobacteria. *Proceedings of the National Academy of Sciences USA* **107**, 19190-19194.

Biddle JF, Lipp JS, Lever MA, Lloyd KG, Sørensen KB, Anderson R, Fredricks HF, Elvert M, Kelly TJ, Schrag DP, Sogin ML, Brenchley JE, Teske A, House CH, Hinrichs K-U (2006) Heterotrophic Archaea dominate sedimentary subsurface ecosystems off Peru. *Proceedings of the National Academy of Sciences USA* **103**, 3846-3851.

D'Hondt SL, Jørgensen BB, Miller DJ, and the Leg 201 shipboard scientific party (2003) *Proceedings of the Ocean Drilling Program, Initial Reports*. Ocean Drilling Program, College Station, TX.

Gutiérrez D, Bouloubassi I, Sifeddine A, Purca S, Goubanova K, Graco M, Field D, Méjanelle L, Velazco F, Lorre A, Salvatteci R, Quispe D, Vargas G, Dewitte B, Ortlieb L (2011) Coastal cooling and increased productivity in the main upwelling zone off Peru since the mid-twentieth century. *Geophysical Research Letters* **38**, L07603.

Hammer Ø, Harper DAT, Ryan PD (2001) PAST: Paleontological Statistics software package for education and data analysis. *Palaeontologica Electronica* **4**, PE4.1.4A.

Hartnett HE, Keil RG, Hedges JI, Devol AH (1998) Influence of

oxygen exposure time on organic carbon preservation in continental margin sediments. *Nature* **391**, 572-574.

Harvey HR, Fallon RD, Patton JS (1986) The effect of organic matter and oxygen on the degradation of bacterial membrane lipids in marine sediments. *Geochimica et Cosmochimica Acta* **50**, 795-804.

Hedges JI, Keil RG (1995) Sedimentary organic matter preservation: an assessment and speculative synthesis. *Marine Chemistry* **49**, 81-115.

Huguet C, Hopmans EC, Febo-Ayala W, Thompson DH, Sinninghe Damsté JS, Schouten S (2006) An improved method to determine the absolute abundance of glycerol dibiphytanyl glycerol tetraether lipids. O*rganic Geochemistry* **37**, 1036-1041.

Jung MY, Park S-J, Min D, Kim J-S, Rijpstra WIC, Sinninghe Damsté JS, Kim G-J, Madsen EL, Rhee S-K (2011) Enrichment and characterization of an autotrophic ammonia-oxidizing archaeon of Mesophilic Crenarchaeal Group I.1a from an Agricultural Soil. *Applied and Environmental Microbiology* **77**, 8635-8647.

Kim J-H, van der Meer J, Schouten S, Helmke P, Willmott V, Sangiorgi F, Koç N, Hopmans EC, Sinninghe Damsté JS (2010) New indices and calibrations derived from the distribution of crenarchaeal isoprenoid tetraether lipids: Implications for past sea surface temperature reconstructions. *Geochimica et Cosmochimica Acta* **74**, 4639-4654.

Koga Y, Morii H (2005) Recent advances in structural research on ether lipids from archaea including comparative and physiological aspects. *Bioscience, Biotechnology, and Biochemistry* **69**, 2019-2034.

Koga Y, Nakano M (2008) A dendrogram of archaea based on lipid component parts composition and its relationship to rRNA phylogeny. *Systematic and Applied Microbiology* **31**, 169-182.

Langworthy TA (1977) Long-chain diglycerol tetraethers from Thermoplasma acidophilum. *Biochimica et Biophysica Acta (BBA) - Lipids and Lipid Metabolism* **487**, 37-50.

Lengger SK, Hopmans EC, Reichart G-J, Nierop KGJ, Sinninghe Damsté JS, Schouten S (2012a) Intact polar and core glycerol dibiphytanyl glycerol tetraether lipids in the Arabian Sea oxygen minimum zone: II. Selective preservation and degradation in sediments and consequences for the TEX_{86}. *Geochimica et Cosmochimica Acta* **98**, 244-258.

Lengger SK, Hopmans EC, Sinninghe Damsté JS, Schouten S (2012b) Comparison of extraction and work up techniques for analysis of core and intact polar tetraether lipids from sedimentary environments. *Organic Geochemistry* **47**, 34-40.

Lengger SK, Kraaij M, Baas M, Tjallingii R, Stuut J-B, Hopmans EC, Sinninghe Damsté JS, Schouten S (2013) Differential degradation of intact polar and core glycerol dialkyl glycerol tetraether lipids upon post-depositional oxidation, *Organic Geochemistry* **65**, 83–93.

Lipp JS, Hinrichs K-U (2009) Structural diversity and fate of intact polar lipids in marine sediments. *Geochimica et Cosmochimica Acta* **73**, 6816-6833.

Lipp JS, Morono Y, Inagaki F, Hinrichs K-U (2008) Significant contribution of Archaea to extant biomass in marine subsurface sediments. *Nature* **454**, 991-994.

Liu X, Lipp JS, Hinrichs K-U (2011) Distribution of intact and core GDGTs in marine sediments. *Organic Geochemistry* **42**, 368-375.

Lloyd KG, Schreiber L, Petersen DG, Kjeldsen KU, Lever MA, Steen AD, Stepanauskas R, Richter M, Kleindienst S, Lenk S, Schramm A, Jørgensen BB (2013). Predominant archaea in marine sediments degrade detrital proteins. *Nature* **496**, 215–218.

Logemann J, Graue J, Köster J, Engelen B, Rullkötter J, Cypionka H (2011) A laboratory experiment of intact polar lipid degradation in sandy sediments. *Biogeosciences* **8**, 2547-2560.

Oba M, Sakata S, Tsunogai U (2006) Polar and neutral isopranyl glycerol ether lipids as biomarkers of archaea in near-surface sediments from the Nankai. *Organic Geochemistry* **37**, 1643-1654.

Pitcher A, Hopmans EC, Mosier AC, Park S-J, Rhee S-K, Francis CA, Schouten S, Sinninghe Damsté JS (2011a) Core and intact polar glycerol dibiphytanyl glycerol tetraether lipids of ammonia-oxidizing archaea enriched from marine and estuarine sediments. *Applied and Environmental Microbiology* **77**, 3468-3477.

Pitcher A, Hopmans EC, Schouten S, Sinninghe Damsté JS (2009) Separation of core and intact polar archaeal tetraether lipids using silica columns: Insights into living and fossil biomass contributions. *Organic Geochemistry* **40**, 12-19.

Pitcher A, Hopmans EC, Villanueva L, Reichart G-J, Schouten S, Sinninghe Damsté JS (2011b) Niche segregation of ammonia-oxidizing archaea and anammox bacteria in the Arabian Sea oxygen minimum zone. *The ISME Journal* **5**, 1896-1904.

Pitcher A, Rychlik N, Hopmans EC, Spieck E, Rijpstra WIC, Ossebaar J, Schouten S, Wagner M, Sinninghe Damsté JS (2010) Crenarchaeol dominates the membrane lipids of Candidatus Nitrososphaera gargensis, a thermophilic Group I.1b Archaeon. *The ISME Journal* **4**, 542-552.

Powell AJ, Dodge JD, Lewis J (1990) Late Neogene to Pleistocene palynological facies of the Peruvian continental margin upwelling, Leg 112. In: *Proceedings of the Ocean Drilling Program, Scientific Results* **112** (eds. Dean WE, Emels K-C, Suess E, Von Huene R). Ocean Drilling Program, College Station, TX, pp. 297–321.

Schouten S, Hopmans EC, Baas M, Boumann H, Standfest S, Könneke M, Stahl DA, Sinninghe Damsté JS (2008) Intact membrane lipids of "Candidatus Nitrosopumilus maritimus," a cultivated representative of the cosmopolitan mesophilic group I crenarchaeota. *Applied and Environmental Microbiology* **74**, 2433-2440.

Schouten S, Hopmans EC, Schefuß E, Sinninghe Damsté JS (2002) Distributional variations in marine crenarchaeotal membrane lipids: a new tool for reconstructing ancient sea water temperatures? *Earth and Planetary Science Letters* **204**, 265-274.

Schouten S, Hopmans EC, Sinninghe Damsté JS (2013) The organic geochemistry of glycerol dialkyl glycerol tetraether lipids: A review. *Organic Geochemistry* **54**, 19-61.

Schouten S, Middelburg JJ, Hopmans EC, Sinninghe Damsté JS (2010) Fossilization and degradation of intact polar lipids in deep subsurface sediments: A theoretical approach. *Geochimica et Cosmochimica Acta* **74**, 3806-3814.

Schouten S, Pitcher A, Hopmans EC, Villanueva L, van Bleijswijk J, Sinninghe Damsté JS (2012) Intact polar and core glycerol dibiphytanyl glycerol tetraether lipids in the Arabian Sea oxygen minimum zone: I. Selective preservation and degradation in the water column and consequences for the TEX_{86}. *Geochimica et Cosmochimica Acta* **98**, 228-243.

Schubotz F, Wakeham SG, Lipp JS, Fredricks HF, Hinrichs K-U (2009) Detection of microbial biomass by intact polar membrane lipid analysis in the water column and surface sediments of the

Black Sea. *Environmental Microbiology* **11**, 2720-2734.

Sinninghe Damsté JS, Rijpstra WIC, Hopmans EC, Jung MY, Kim JG, Rhee SK, Stieglmeier M, Schleper C (2012) Intact polar and core dibiphytanyl glycerol tetraether lipids of group I. 1a and I. 1b thaumarchaeota in soil. *Applied and Environmental Microbiology* **78**, 6866-6874.

Sinninghe Damsté JS, Rijpstra WIC, Reichart G-J (2002a) The influence of oxic degradation on the sedimentary biomarker record II. Evidence from Arabian Sea sediments. *Geochimica et Cosmochimica Acta* **66**, 2737-2754.

Sinninghe Damsté JS, Schouten S, Hopmans EC, van Duin ACT, Geenevasen JAJ (2002b) Crenarchaeol: the characteristic core glycerol dibiphytanyl glycerol tetraether membrane lipid of cosmopolitan pelagic crenarchaeota. *Journal of Lipid Research* **43**, 1641-1651.

Skilbeck CG, Fink D (2006) Data report: Radiocarbon dating and sedimentation rates for Holocene upper Pleistocene sediments, eastern equatorial Pacific and Peru continental margin. In: *Proceedings of the Ocean Drilling Program, Scientific Results* **201** (eds. Jørgensen BB, D'Hondt SL, and Miller DJ). Ocean Drilling Program, College Station, TX, pp. 1-15.

Weijers JWH, Lim KL, Aquilina A, Sinninghe Damsté JS, Pancost RD (2011) Biogeochemical controls on glycerol dialkyl glycerol tetraether lipid distributions in sediments characterized by diffusive methane flux. *Geochemistry Geophysics Geosystems* **12**, Q10010.

Woese CR, Fox GE (1977) Phylogenetic structure of the prokaryotic domain: The primary kingdoms. *Proceedings of the National Academy of Sciences USA* **74**, 5088-5090.

Xie S, Lipp JS, Wegener G, Ferdelman TG, Hinrichs K-U (2013) Turnover of microbial lipids in the deep biosphere and growth of benthic archaeal populations. *Proceedings of the National Academy of Science USA* **110**, 6010–6014.

Zhu C, Lipp JS, Wörmer L, Becker KW, Schröder J, Hinrichs K-U (2013) Comprehensive glycerol ether lipid fingerprints through a novel reversed phase liquid chromatography–mass spectrometry protocol. *Organic Geochemistry* **65**, 53–62.

Supporting information. Raw data of organic carbon and lipid concentrations have been archived and are available at http://doi.pangaea.de/10.1594/PANGAEA.828778 and from the supplied file: supp_info.csv. Supplementary figures S1-S3 are supplied and described in file supp_figures.pdf, to be found under http://onlinelibrary.wiley.com/doi/10.1111/gbi.12081/suppinfo .

Supplementary figure captions.

Figure S1. Concentrations vs. depth (mbsf) of (a) CL-GDGTs in μg . g C_{org}^{-1}, (b) IPL-derived GDGTs in μg . g C_{org}^{-1} and (c) IPL-crenarchaeol with MH-, DH- and HPH-headgroups (in area . g C_{org}^{-1}) and and (d) C_{org}. in mg . g sed dw^{-1}.

Figure S2. Results of the principal component analysis of the concentrations and abundances of C_{org}, CL- and IPL-GDGTs and IPL-crenarchaeol. (a) scores plot, (b) loadings plot.

Figure S3. Correlation of IPL-derived TEX_{86} with CL-TEX_{86}. IPL-TEX_{86} = 0.618 + 0.162 . CL-TEX_{86} (R^2 = 0.013; P = 0.6177).

Supplementary figures S1-S3 to:

Fossilization and degradation of archaeal intact polar tetraether lipids in deeply-buried marine sediments (Peru Margin)

Sabine K. Lengger [#, *] , Ellen C. Hopmans, Jaap S. Sinninghe Damsté and Stefan Schouten

Geobiology, 2014.

Department of Marine Organic Biogeochemistry, Royal NIOZ Netherlands Institute for Sea Research, P. O. Box 59, 1790AB Den Burg, Texel, The Netherlands.

Present address: Petroleum & Environmental Geochemistry Group, Biogeochemistry Research Centre, Plymouth University, Drake Circus, Plymouth, Devon, PL4 8AA, UK.

*Corresponding author. E-mail address: sabine.lengger@plymouth.ac.uk

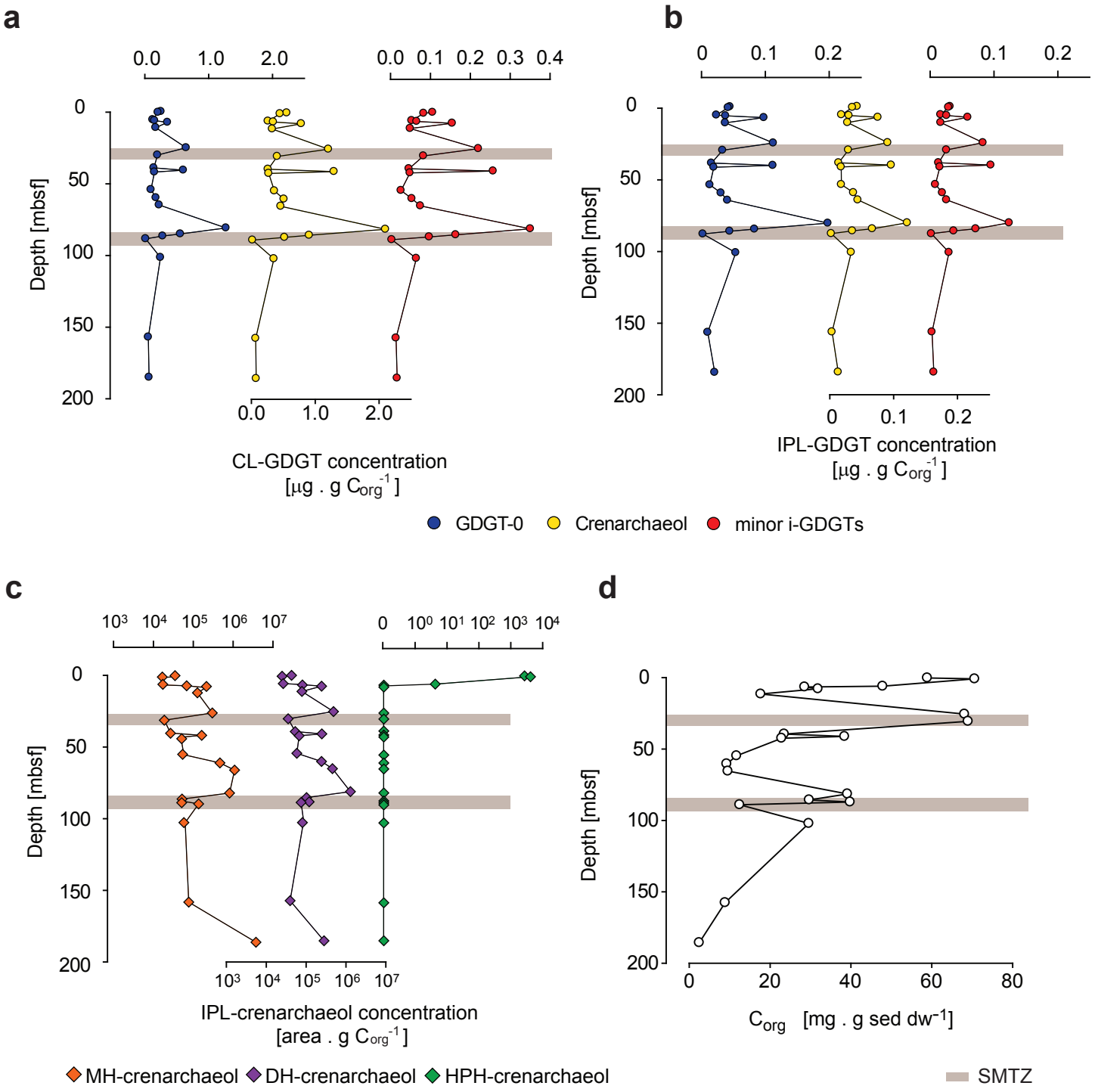

Figure S1. Concentrations vs. depth (mbsf) of (a) CL-GDGTs in µg . C_{org}^{-1}, (b) IPL-derived GDGTs in µg . g g C_{org}^{-1} and (c) IPL-crenarchaeol with MH-, DH- and HPH-headgroups (in area . g C_{org}^{-1}) and and (d) C_{org}. in mg . g sed dw^{-1}.

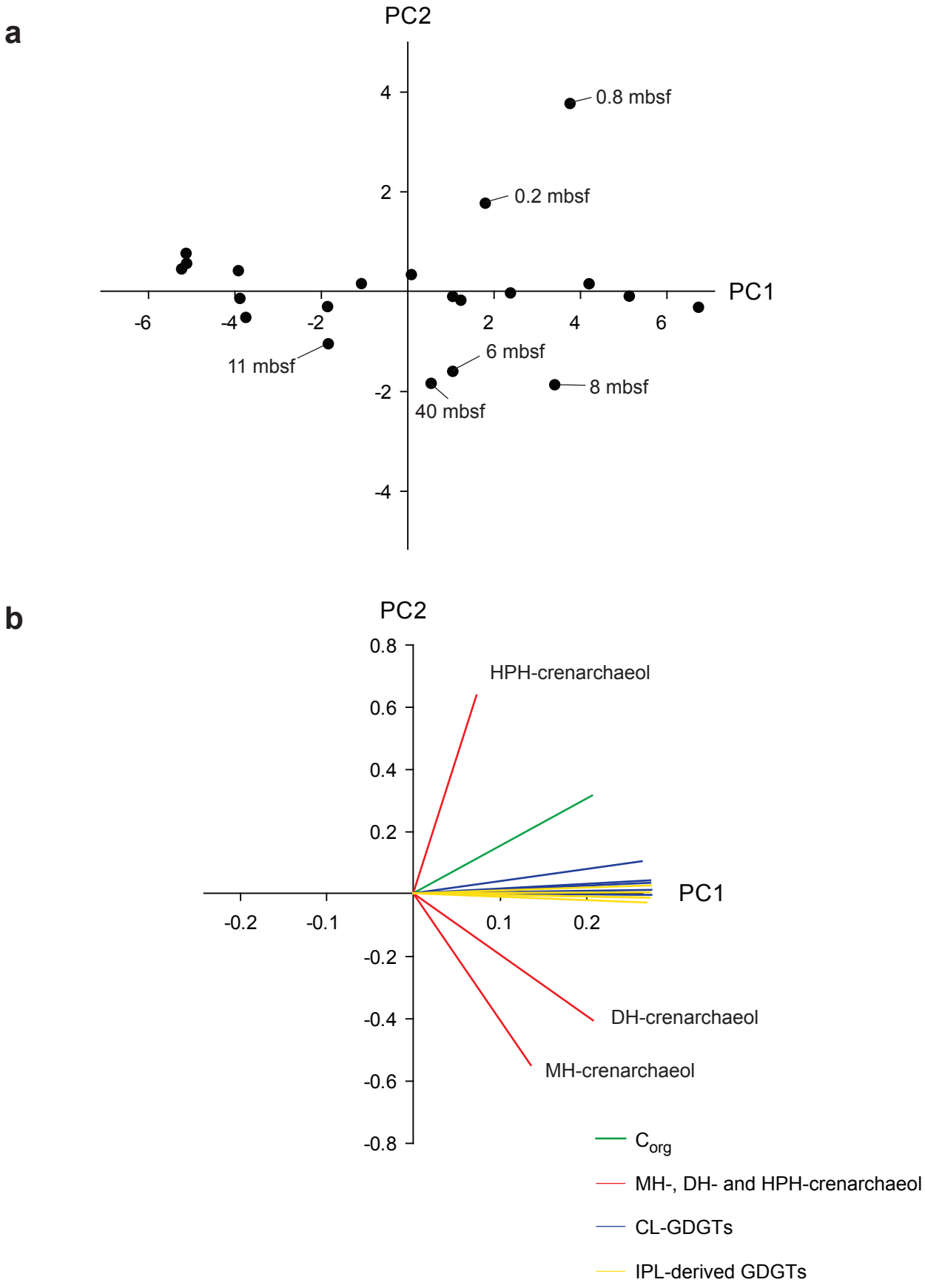

Figure S2. Results of the principal component analysis of the concentrations and abundances of C_{org}, CL- and IPL-GDGTs and IPL-crenarchaeol. (a) scores plot, (b) loadings plot.

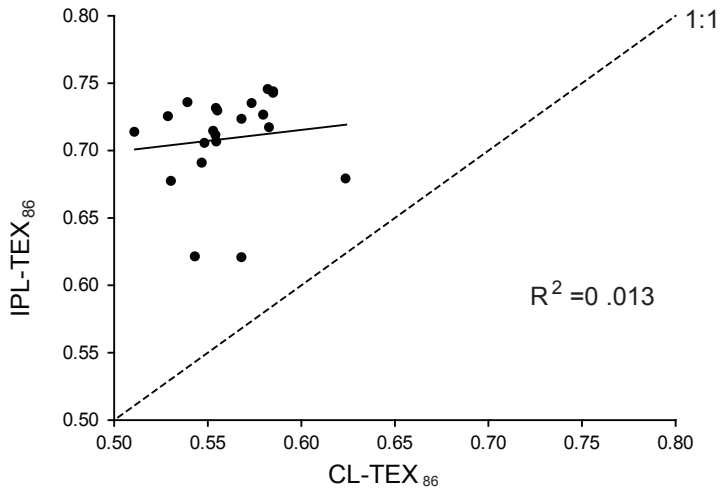

Figure S3. Correlation of IPL-derived TEX_{86} with CL-TEX_{86}. IPL-TEX_{86} = 0.618 + 0.162 × TEX_{86} (R^2 = 0.013; P = 0.6177).